

THE RADIO EMISSION FROM THE TYPE Ic SUPERNOVA SN 1990B

SCHUYLER D. VAN DYK¹

Center for Advanced Space Sensing, Naval Research Laboratory, Code 7215, Washington, DC 20375-5351

RICHARD A. SRAMEK

P.O. Box 0, National Radio Astronomy Observatory, Socorro, NM 87801

KURT W. WEILER

Center for Advanced Space Sensing, Naval Research Laboratory, Code 7215, Washington, DC 20375-5351

AND

NINO PANAGIA^{2,3}

Space Telescope Science Institute, 3700 San Martin Drive, Baltimore, MD 21218

Received 1992 August 10; accepted 1992 October 27

ABSTRACT

We present radio observations of the Type Ic (“helium-poor” Type Ib) supernova SN 1990B in NGC 4568 made with the Very Large Array at 20, 6, 3.6, and 2 cm from 1990 February through 1990 October. We find that its radio properties are quite similar to those of the two previously known Type Ib radio supernovae, SN 1983N and SN 1984L, and clearly distinguishable from the radio emission from Type II radio supernovae such as SN 1979C and SN 1986J. Nevertheless, there appear to be smaller, albeit significant, differences in the radio emission and physical properties of Type Ic from Type Ib radio supernovae. We discuss the radio properties of SN 1990B in the context of progenitor models for the Types Ib/c supernovae and conclude that an interacting binary system origin remains the most promising model. Finally, we suggest that Type Ib, and perhaps Ib/c, radio supernovae may form a class of radio “standard candles” which could be useful as distance indicators.

Subject headings: galaxies: individual (NGC 4568) — radio continuum: stars — supernovae: individual (SN 1990B)

1. INTRODUCTION

Supernovae (SNs, hereafter) which are significant sources of radio emission have been referred to as “radio SNs” (RSNs, hereafter). These objects provide important information about the nature of the progenitor stellar systems and their immediate circumstellar environments, as well as on the connection between SNs, RSNs, and supernova remnants (see Weiler et al. 1986; Weiler & Sramek 1988). So far, Type Ib SNs and Type II SNs appear to be radio emitters, while the Type Ia SNs are not detected to the sensitivity limits of the Very Large Array (VLA).⁴

The Type Ib SNs 1983N in NGC 5236 (M83) and 1984L in NGC 991 were found to be RSNs with very similar behavior in terms of their observed radio light curves (see Weiler et al. 1986; Panagia, Sramek, & Weiler 1986). This behavior has been shown to be distinct relative to the behavior of the radio light curves of the Type II RSNs (Weiler et al. 1986; Weiler & Sramek 1988; Van Dyk et al. 1993). This implies that the circumstellar environments of Type Ib RSNs are significantly different from those of the Type II RSNs, which further implies a difference in the progenitor stellar systems.

Since the detection and monitoring in the optical and radio of SNs 1983N and 1984L, the level of understanding about the

nature of the Type Ib SNs has increased. Based on the strength of the helium absorption line present in their early-time optical spectra, the Type Ib SNs appear to bifurcate into apparent subtypes, the “helium-rich” Type Ib SNs and the “helium-poor” Type Ic SNs (e.g., see Wheeler & Harkness 1990). However, the fact that their late-time spectra are very similar continues to indicate that the two subclasses are closely related (Wheeler & Harkness 1990; Filippenko 1991a) and may not actually represent different phenomena. We will therefore often refer to both possible subtypes as Ib/c in this paper.

We discuss in this paper the radio emission from SN 1990B in NGC 4568. The SN was discovered by Perlmutter & Pennypacker (1990) at magnitude 16 on five images obtained between 1990 January 20.47 and 21.51 UT as part of the Berkeley Automated Supernova Search. Perlmutter & Pennypacker had not detected the SN to limiting magnitude 18 on 1989 December 23. From spectra taken on 1990 January 23 and 24, respectively, Filippenko (1990) and Kirshner & Leibundgut (1990) each concluded that SN 1990B was Type Ib. Benetti, Cappellaro, & Turatto (1990) also confirmed this classification based on a spectrum taken on 1990 February 20. Filippenko suggested that the spectrum of SN 1990B closely resembled the spectrum of SN 1987M, a Type Ic SN, several weeks past maximum. He found that the helium absorption lines for SN 1990B were weak or absent, making this SN an example of a “helium-weak” Type Ib, i.e., a Type Ic SN. SN 1990B was apparently heavily reddened, as indicated by the presence of strong narrow interstellar Na D lines in its spectrum (Filippenko 1990; Dopita & Ryder 1990; Benetti et al. 1990) and the lack of detection of the SN with the *IUE* (Panagia et al. 1990).

¹ Naval Research Laboratory/National Research Council Cooperative Research Associate.

² Affiliated with the Astrophysics Division, Space Science Department of ESA.

³ Also University of Catania, Italy.

⁴ The VLA is operated by the National Radio Astronomy Observatory of Associated Universities, Inc., under a cooperative agreement with the National Science Foundation.

TABLE 1
GENERAL PROPERTIES OF SN 1990B AND NGC 4568

Property (1)	Value (2)
SN 1990B	
R.A. (1950.0)	$12^{\text{h}}34^{\text{m}}02^{\text{s}}.167 \pm 0^{\text{s}}.01$
Decl. (1950.0)	$+11^{\circ}31'00''.22 \pm 0''.2$
SN type	Ic
Date of optical maximum ^a	$\sim 1990 \text{ Jan } 18$
Apparent V magnitude of optical maximum ^b	$\lesssim 16.0$
(uncorrected for reddening)	
Absolute V magnitude of optical maximum ^{c, d}	$\lesssim -17.1$
(corrected for reddening)	
Maximum observed radio flux density (6 cm)	$1.04 \pm 0.08 \text{ mJy}$
Maximum observed spectral luminosity (6 cm) ^d	$\sim 3.5 \times 10^{26} \text{ ergs s}^{-1} \text{ Hz}^{-1}$
Maximum observed flux density ratio to Cas A (6 cm)	~ 50
NGC 4568	
Galaxy type	Sc
Heliocentric velocity	2320 km s^{-1}
Galaxy distance ^d	16.8 Mpc

^a Estimated; cf. § 2.

^b Suntzeff 1990; Suntzeff & Phillips 1990.

^c Adopting a lower limit to the reddening of $A_V > 2$ (Panagia et al. 1990).

^d Distance to NGC 4568 of 16.8 Mpc from Tully 1988 with $H_0 = 75 \text{ km s}^{-1} \text{ Mpc}^{-1}$.

The SN was first detected in the radio with the VLA as a 1.0 mJy source at 20 cm on 1990 February 13 by Sramek, Weiler, & Panagia (1990) at $\alpha(1950.0) = 12^{\text{h}}34^{\text{m}}02^{\text{s}}.167 \pm 0^{\text{s}}.01$, $\delta(1950.0) = +11^{\circ}31'00''.22 \pm 0''.2$, which is coincident to within the errors with its optical position ($\alpha[1950.0] = 12^{\text{h}}34^{\text{m}}02^{\text{s}}.2$, $\delta[1950.0] = +11^{\circ}30'59''$; Dopita & Ryder 1990). We present in this paper the results of our monitoring with the VLA of this supernova at wavelengths 20, 6, 3.6, and 2 cm and provide the complete radio light curves for SN 1990B, as well as an interpretation of the data in terms of possible progenitor systems. We summarize in Table 1 the general properties of SN 1990B and its parent galaxy NGC 4568.

2. TIME OF OPTICAL MAXIMUM

An exact date of optical maximum for SN 1990B cannot be readily determined from the various reports given in the IAU Circulars. However, several investigators have offered their estimates of the time of optical maximum, and these are listed in Table 2.

Examination of Table 2 shows that almost any date between 1990 January 1 and February 6 is suggested by optical observers. However, the brightest V magnitude recorded for SN 1990B was $V = 16.06$ by Suntzeff (1990) on 1990 January

24.33, with the SN declining rapidly after that date. Therefore, an optical maximum date later than 1990 January 24 is not credible. Also, only Filippenko (1990), examining the unreduced data of H. Spinrad & M. Dickinson, suggests an optical maximum date as early as 1990 January 1 or earlier. The more general consensus drawn from the observations listed in Table 2 is for an optical maximum date in the interval 1990 January 14 through January 23. We therefore adopt a date of $\sim 1990 \text{ January } 18 \pm 1 \text{ week}$ as the epoch of optical maximum for SN 1990B throughout this paper. Such a date is not inconsistent with the lack of optical detection by Perlmutter & Pennypacker (1990) at $\sim 18^{\text{m}}$ on 1989 December 23, since Type Ib/c optical light curves are known to steeply rise to maximum brightness in only a few days ($\sim 4^{\text{m}}$ in $\sim 12 \text{ days}$; see Figure 3.2 of Kirshner 1990).

3. RADIO OBSERVATIONS

The radio observations of SN 1990B were made with the VLA at 20 cm (1.490 GHz), 6 cm (4.860 GHz), 3.6 cm (8.440 GHz), and 2 cm (14.940 GHz) from 1990 February 1 through 1990 October 10. Since monitoring of an evolving radio source requires measurement at frequent intervals, we were not able

TABLE 2
ESTIMATES OF THE DATE OF OPTICAL MAXIMUM FOR SN 1990B

Estimate for Date of Maximum (1)	Range of Dates (2)	Technique (3)	Reference (4)
$\sim 2\text{--}4$ weeks before 1990 Feb 20	1990 Jan 23–Feb 6	Spectroscopy	1
1990 Jan 17 ± 3 days	1990 Jan 14–Jan 20	Photometry	2
~ 1 week before 1990 Jan 24	$\sim 1990 \text{ Jan } 17$	Spectrophotometry	3
“Several weeks past maximum” on 1990 Jan 23	$\sim 1990 \text{ Jan } 1\text{--}16$	Spectroscopy	4
Near maximum on 1990 Jan 24	$\sim 1990 \text{ Jan } 24$	Spectroscopy	5
$\equiv 1990 \text{ Jan } 18 \pm 1 \text{ week}$	1990 Jan 11–Jan 25	Average	6

REFERENCES.—(1) Benetti et al. 1990; (2) Suntzeff & Phillips 1990; (3) Phillips & Ruiz 1990; (4) Filippenko 1990; (5) Kirshner & Leibundgut 1990; (6) Present work (cf. § 2).

TABLE 3
CALIBRATION SOURCES

Source Name (1)	Calibrator Type (2)	$\alpha_{1950.0}$ (3)	$\delta_{1950.0}$ (4)	S_{20} (Jy) (5)	S_6 (Jy) (6)	$S_{3.6}$ (Jy) (7)	S_2 (Jy) (8)
3C 286	Primary	Not used	Not used	14.52	7.55	5.27	3.50
1219 + 285 ^a	Secondary	12 ^h 19 ^m 01 ^s .120	+28°30'26".45

^a See Table 4 for flux densities.

to request the specific VLA configuration and consequently have measurements at various array sizes. However, we were fortunate that many of the observations were made at the largest VLA configuration, A-array, where confusion from the extended emission of the parent galaxy is at a minimum. By 1990 October 10, the RSN had become sufficiently weak at all four monitoring wavelengths that detection was impossible with reasonable integration times, so observations were halted. Along with each observation of SN 1990B, a short observation of a "secondary," possibly variable, calibrator, 1219 + 285, was made at each frequency. To establish an absolute flux density scale, most observing sessions also included an observation of the "primary," presumed constant, flux density calibrator 3C 286.

3.1. Calibration

The VLA is described in a number of publications (e.g., Thompson et al. 1980; Hjellming & Bignell 1982; Napier, Thompson, & Ekers 1983); the general procedures for RSN observations, with analysis of the possible sources of error, are discussed in Weiler et al. (1986). The "primary" calibrator employed here, 3C 286, was assumed to be constant in flux density with time and to have the flux densities at 20, 6, 3.6, and 2 cm given in Table 3.

The "secondary" calibrator, 1219 + 285, was used as the phase (position) and amplitude (flux density) reference for the observations of SN 1990B. Its assumed position (epoch 1950.0) is given in Table 3, and its flux density values, measured against 3C 286, at 20 cm (S_{20}), 6 cm (S_6), 3.6 cm ($S_{3.6}$), and 2 cm (S_2) are presented for each observing date in Table 4. On five separate epochs (1990 February 6, 1990 February 18, 1990 February 26, 1990 March 14, and 1990 October 10) independent calibrations with 3C 286 were not available, and other means, described in the footnotes to Table 4, were employed for determining calibration values.

3.2. Data Reduction

The data were initially calibrated using standard software packages within AIPS on the Convex computers at the VLA and, after "export" to the NRL, using the local IBM RS/6000 computer. The data were further analyzed, after calibration, at the VLA and at NRL. All data sets were edited, CLEANed, imaged using both IF channels, and measured.

3.3. Errors

One estimate for the flux density measurement error is the rms of the fluctuations in the background of the image. This is only a lower limit to the total error. Therefore, errors for the measurements in this paper also include a basic 5% error to account for inaccuracies in the flux density calibration and any absolute scale error for the primary calibrator, 3C 286. The

final errors, σ_f , listed in Table 5, are taken as

$$\sigma_f^2 \equiv (0.05S_0)^2 + \sigma_0^2, \quad (1)$$

where S_0 is the observed flux density for SN 1990 B and σ_0 is the observed rms fluctuations measured on the image outside of any obvious regions of emission.

Since most of the observations were made in the A-array configuration, the disk emission of NGC 4568 was highly resolved out, and it was not necessary to subtract background emission due to the parent galaxy from the measured flux density per beam area of the SN. For three observing epochs (1990 August 24, 1990 September 26, and 1990 October 10), however, the array configurations were more compact (i.e., shorter baselines and lower resolving power), so that the SN emission at 20 cm was too confused by this disk emission of NGC 4568 to detect the SN. Only 3 σ upper limits to detection could be established at those times. On 1990 February 1, the VLA was in its most compact configuration (D-array), so that disk emission was a severe problem at all wavelengths, and only very crude upper limits to the SN flux density could be established.

TABLE 4
MEASURED^a OR ASSUMED FLUX DENSITY VALUES
FOR THE SECONDARY CALIBRATOR 1219 + 285

Observation Date (1)	S_{20} (Jy) (2)	S_6 (Jy) (3)	$S_{3.6}$ (Jy) (4)	S_2 (Jy) (5)
1990 Feb 1	1.02	0.99	1.04
1990 Feb 6	1.063 ^b	...
1990 Feb 13	1.002	1.075	1.063	1.066
1990 Feb 18	0.996 ^c	1.049 ^c	1.035 ^c	1.066 ^c
1990 Feb 26	0.996 ^c	1.049 ^c	1.035 ^c	1.066 ^c
1990 Mar 7	0.989	1.022	1.007	...
1990 Mar 15	1.001 ^d	1.032 ^d	1.025 ^d	...
1990 Apr 26	1.012	1.042	1.042	...
1990 May 29	0.976	0.995
1990 Jun 29	0.989	1.007
1990 Aug 24	0.998
1990 Sep 26	0.980
1990 Oct 10	0.980 ^e

^a Independently calibrated using 3C 286.

^b Not independently calibrated. Calibration value adopted from 1990 February 13.

^c Not independently calibrated. Calibration values taken as an average of the results on 1990 February 13 and 1990 March 7.

^d Not independently calibrated. Calibration values taken as an average of the results on 1990 March 7 and 1990 April 26.

^e Not independently calibrated. Calibration value adopted from 1990 September 26.

TABLE 5
FLUX DENSITY MEASUREMENTS FOR SN 1990B

OBSERVATION DATE (1)	TIME SINCE OPTICAL MAXIMUM ^a (days) (2)	VLA CONFIGURATION (3)	FLUX DENSITY						
			S_{20} (mJy) (4)	σ_{20} (mJy) (5)	S_6 (mJy) (6)	σ_6 (mJy) (7)	$S_{3.6}$ (mJy) (8)	$\sigma_{3.6}$ (mJy) (9)	S_2 (mJy) (10)
1990 Jan 18	$\equiv 0$		<13.5 ^b	...	<4.9 ^b	...	<1.65 ^b
1990 Feb 1	14	D	0.60	0.06	...
1990 Feb 6	19	D/A
1990 Feb 13	26	A	0.83	0.11	1.01	0.09	0.37	0.06	<0.60 ^c
1990 Feb 18	31	A	1.32	0.12	1.04	0.08	0.56	0.06	<0.54 ^c
1990 Feb 26	39	A	1.24	0.12	0.84	0.07	0.43	0.05	<0.51 ^c
1990 Mar 7	48	A	1.48	0.11	0.74	0.07	0.38	0.05	...
1990 Mar 14	56	A	1.45	0.13	0.75	0.07	0.39	0.04	...
1990 Apr 26	98	A	1.18	0.15	0.50	0.07	0.25	0.04	...
1990 May 29	131	A	1.04	0.12	0.25	0.06
1990 Jun 29	162	A/B	0.85	0.19	0.27	0.06
1990 Aug 24	218	B	<0.87 ^c
1990 Sep 26	251	B/C	<1.02 ^c
1990 Oct 10	265	C	<1.08 ^c

^a The date of optical maximum is taken to be 1990 January 18 (see § 2) and the date of explosion is taken to be 1989 December 15, 35 days before optical maximum (see § 5).

^b The radio emission from the SN could not be resolved from the nucleus of NGC 4568, so that only crude upper limits could be established.

^c 3 σ upper limit.

4. RESULTS

We present the results of our flux density measurements at 20, 6, 3.6, and 2 cm in Table 5. Column (1) is the date of observation; column (2) is the time, in days, since the assumed date of optical maximum (see § 2); column (3) gives the VLA configuration in which the supernova was observed; columns (4), (6), and (8) give the measured flux densities at 20 cm (S_{20}), 6 cm (S_6), and 3.6 cm ($S_{3.6}$), respectively; and columns (5), (7), and (9) give the error estimates for these measurements. It was only possible to place 3 σ upper limits to the detection of 2 cm emission from the SN, and these are given in column (10) of Table 5.

Since the flux densities at 6 and 3.6 cm were only ~ 0.25 mJy on 1990 April 25 and 1990 June 29, respectively, and rapidly declining, we halted further observations at these two wavelengths. In addition, since after 1990 June 29 the VLA was

scheduled for more compact configurations, for which confusion with background emission from the parent galaxy is a much greater problem, and since measurement attempts on 1990 August 24, 1990 September 26, and 1990 October 10 all resulted in nondetections, all monitoring was terminated. Because such a rapidly declining SN was unlikely to still be detectable when the VLA returned to A-array in ~ 1991 June, the observations given in Table 5 almost certainly represent the complete data set for the radio emission from SN 1990B.

We present in Table 6 determinations of the spectral index, α , from our data ($S \propto \nu^{+\alpha}$). Columns (1) and (2) are the same as in Table 5. Column (3) lists the spectral index, α_6^{20} , between 20 and 6 cm, and column (4), its error, $\sigma_{\alpha_6^{20}}$; column (5) lists the spectral index, $\alpha_{3.6}^{20}$, between 20 and 3.6 cm, and column (6), its error, $\sigma_{\alpha_{3.6}^{20}}$; column (7) lists the spectral index, $\alpha_{3.6}^6$, between 6 and 3.6 cm, and column (8), its error, $\sigma_{\alpha_{3.6}^6}$.

TABLE 6
SPECTRAL INDEX MEASUREMENTS FOR SN 1990B

OBSERVATION DATE (1)	TIME SINCE OPTICAL MAXIMUM ^a (days) (2)	SPECTRAL INDEX ($S \propto \nu^{+\alpha}$)					
		α_6^{20} (3)	$\sigma_{\alpha_6^{20}}$ (4)	$\alpha_{3.6}^{20}$ (5)	$\sigma_{\alpha_{3.6}^{20}}$ (6)	$\alpha_{3.6}^6$ (7)	$\sigma_{\alpha_{3.6}^6}$ (8)
1990 Jan 18	$\equiv 0$
1990 Feb 1	14
1990 Feb 6	19
1990 Feb 13	26	0.17	0.13	-0.47	0.12	-1.82	0.34
1990 Feb 18	31	-0.20	0.10	-0.49	0.08	-1.12	0.23
1990 Feb 26	39	-0.33	0.11	-0.61	0.08	-1.21	0.25
1990 Mar 7	48	-0.59	0.10	-0.78	0.09	-1.21	0.31
1990 Mar 14	56	-0.56	0.11	-0.76	0.08	-1.18	0.27
1990 Apr 26	98	-0.73	0.15	-0.89	0.12	-1.26	0.38
1990 May 29	131	-1.21	0.23
1990 Jun 29	162	-0.97	0.27

^a The date of optical maximum is taken to be 1990 January 18 (see § 2) and the date of explosion is taken to be 1989 December 15, 35 days before optical maximum (see § 5).

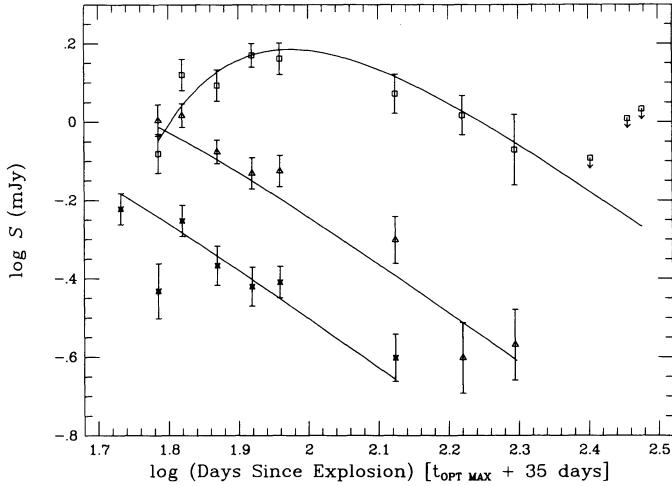


FIG. 1.—Radio “light curves” for SN 1990B in NGC 4568. The three wavelengths, 20 cm (open squares), 6 cm (open triangles), and 3.6 cm (four-sided stars), are shown together. The age of the supernova is measured in days from the estimated date of explosion on 1989 December 15 (35 days before the estimated date of optical maximum on 1990 January 18). The solid lines represent the best-fit light curves of the form $S(\text{mJy}) = K_1 \left[\frac{\nu}{5 \text{ GHz}} \right]^\alpha \left[\frac{t - t_0}{1 \text{ day}} \right]^\beta e^{-\tau}$, where $\tau = K_2 \left[\frac{\nu}{5 \text{ GHz}} \right]^{-2.1} \left[\frac{t - t_0}{1 \text{ day}} \right]^\delta$, and $\delta \equiv \alpha - \beta - 3$.

In Figure 1 we plot the time evolution of the flux density of SN 1990B in all three radio bands for which we have actual detections (the 2 cm upper limits are omitted). The solid lines are the “best-fit” model light curves discussed below. In Figure 2 we show the time evolution of the spectral indices, $\alpha_{6,20}^0$, $\alpha_{3.6,20}^0$, and $\alpha_{3.6,6}^0$. The solid curves shown in Figure 2 are not independent fits but are calculated from the model light curves shown in Figure 1.

5. MODEL RADIO LIGHT CURVES

It has been shown (see, e.g., Weiler et al. 1986) that the radio light curves for all known RSNs (with the notable exception of

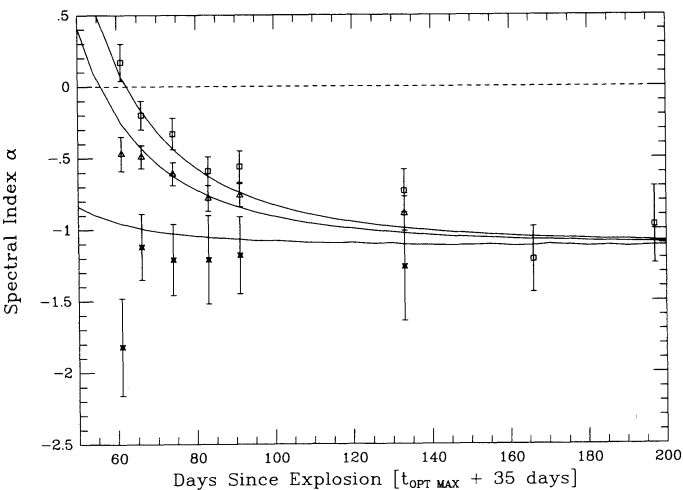


FIG. 2.—The evolution of the spectral indices α ($S \propto \nu^\alpha$) for SN 1990B between 20 and 6 cm (open squares), 20 and 3.6 cm (open triangles), and 6 and 3.6 cm (four-sided stars), plotted as a function of time, in days, since the estimated explosion date of 1989 December 15 (35 days before the estimated date of optical maximum on 1990 January 18). The solid lines are not independently fit but are calculated from the best-fit theoretical “light curves” shown in Fig. 1. The dashed line shows $\alpha = 0$.

SN 1986J; see Weiler, Panagia, & Sramek 1990) can be adequately modeled by a relation of the form:

$$S(\text{mJy}) = K_1 \left(\frac{\nu}{5 \text{ GHz}} \right)^\alpha \left(\frac{t - t_0}{1 \text{ day}} \right)^\beta e^{-\tau}, \quad (2)$$

where

$$\tau = K_2 \left(\frac{\nu}{5 \text{ GHz}} \right)^{-2.1} \left(\frac{t - t_0}{1 \text{ day}} \right)^\delta. \quad (3)$$

The factors K_1 and K_2 above are scaling parameters for the units of choice (mJy, GHz, and days) and formally correspond to the flux density and optical depth, respectively, at 5 GHz, 1 day after explosion. This formulation assumes (1) that the radio emission is due to the nonthermal synchrotron process with optically thin spectral index, α ; (2) that the absorption or optical depth, τ , is purely of a thermal, free-free nature in an ionized medium (frequency dependence $\nu^{-2.1}$) external to the emitting region with a radial density dependence $\rho \propto r^{-2}$ from a red supergiant (RSG) wind of constant speed; and (3) that the observed flux density S , and the optical depth, τ , can be well described as functions of supernova age, $t - t_0$, to the powers β and δ , respectively, after an explosion epoch t_0 .

The detected flux densities at 20, 6, and 3.6 cm were used to solve for the five free parameters, K_1 , K_2 , α , β , and t_0 in equations (2) and (3). In previous work the radio emission from RSNs has been successfully interpreted using the Chevalier “minishell” model (e.g., Chevalier 1981a, b; 1984a, b; see also Weiler et al. 1986, 1990, 1991), which postulates the external generation of relativistic electrons and enhanced magnetic field necessary for synchrotron radio emission by the shock wave from the supernova explosion interacting with a relatively dense circumstellar cocoon of matter. This cocoon is assumed to have been created by mass loss in a stellar wind from a RSG star before the explosion. Because of this model’s success, the parameter δ was not solved for, but was taken to be (Chevalier 1984b)

$$\delta \equiv \alpha - \beta - 3. \quad (4)$$

The best fit for the model radio light curves was obtained by using a minimum reduced χ_{red}^2 procedure to identify the best value and range of values for each of the parameters. Even after having established a probable date for optical maximum (see § 2), the epoch of explosion, t_0 , still remains unknown. In order to estimate it, a series of model fits were performed for a number of possible explosion dates, and an initial epoch of ~ 35 days before optical maximum yielded the best fit to the available data as determined by the minimum χ_{red}^2 . We therefore define $t_0 \equiv 1989$ December 15, 35 days before the date of optical maximum which is estimated to have occurred on 1990 January 18.

The parameter values obtained from the radio data are listed in Table 7. A minimum value of $\chi_{\text{red}}^2 \simeq 1.1$ indicates that the model we are using is a good description of the available data within the known and estimated measurement errors. The range of uncertainty listed for each parameter in Table 7 is the amount that the parameter must deviate from the best-fit value in order to increase χ_{red}^2 from ~ 1 to ~ 5 (Abramowitz & Stegun 1965). This is appropriate for a four-parameter fit (t_0 remained fixed in the fitting) and determines the 67% probability intervals within which the true values lie; that is, the error range analogous to the 1σ uncertainty for a single parameter fit. The model curves calculated with equations (2) and (3) for

TABLE 7
FITTING PARAMETERS FOR SN 1990B^a

Parameter (1)	Value (2)	Deviation Range ^b (3)
K_1	198	158–240
α	-1.12	-(1.04–1.19)
β	-1.27	-(1.24–1.31)
K_2	1.48×10^4	$(0.98–2.25) \times 10^4$
δ ($\equiv \alpha - \beta - 3$) ..	-2.85	-(2.73–2.95)
t_0^c	\equiv 1989 Dec 15	1989 Nov 29–1989 Dec 26
\dot{M}^d ($M_\odot \text{ yr}^{-1}$) ...	1.7×10^{-6}	

^a The radio light curves are assumed to fit a curve of the form: $S(\text{mJy}) = K_1 [v/5 \text{ GHz}]^\alpha [(t - t_0)/(1 \text{ day})]^\beta e^{-\tau}$, where $\tau = K_2 [v/5 \text{ GHz}]^{-2.1} [(t - t_0)/(1 \text{ day})]^\delta$. From Chevalier (1984b), $\delta \equiv \alpha - \beta - 3$ is assumed.

^b The Deviation Range is the range in which there is a $\sim 67\%$ probability that the true value lies. This is equivalent to a 1σ range for a one-parameter solution.

^c The date of the explosion is taken to be 1989 December 15, 35 days before the estimated date of optical maximum on 1990 January 18 (see §§ 2 and 5).

^d The mass-loss rate \dot{M} was calculated using eq. (16) of Weiler et al. (1986) assuming an RSG wind velocity $w = 10 \text{ km s}^{-1}$, ejecta expansion velocity $v_i = 10^4 \text{ km s}^{-1}$ on day $t_i = 45$ days, and a RSG wind temperature $T = 10^4 \text{ K}$. The parameter m is defined in § 6.3, and the optical depth at 5 GHz, $\tau_{5 \text{ GHz}}$, is taken to be K_2 on $t - t_0 = 1$ day.

the parameter values of Table 7 are shown as the solid lines in Figure 1.

Examination of Figure 1 shows that the curves, even for such a simple model, describe the available data at all frequencies very well in gross terms. The only significant deviation is that of the 3.6 cm observation on 1990 February 13, which lies more than 2σ below the model curve at that wavelength.

One can see from Figure 2 that the changes in the spectral indices α_6^{20} , $\alpha_{3.6}^{20}$, and $\alpha_{3.6}^6$ are all well behaved as expected, becoming more negative with time, as the absorbing gas becomes optically thin at progressively lower frequencies. All three spectral indices asymptotically approach a common negative value of $\alpha \sim -1.2$ by ~ 200 days after explosion.

6. DISCUSSION

6.1. The Nature of SN 1990B

If one assumes that the dense circumstellar cocoon required by the Chevalier minishell model to account for the radio emission and absorption observed for SN 1990B was established by a high-density presupernova stellar wind, the stellar mass-loss rate can be estimated using the simplified formula of equation (16) in Weiler et al. (1986). Denoting the wind velocity as w and assuming that the optical expansion velocity of the SN ejecta, v_i , and the electron temperature in the wind (assumed to be equivalent to the excitation temperature), T , for SN 1990B are 10^4 km s^{-1} and 10^4 K , respectively, at $t_i = 45$ days (note that these values are similar to those modeled for the optical observations of the Type Ic SN 1987M in NGC 2715 [$v_i \simeq 1.1 \times 10^4 \text{ km s}^{-1}$, $T \sim 8.5 \times 10^3 \text{ K}$]; Jeffery et al. 1991), and that the optical depth $\tau_{5 \text{ GHz}} = K_2$ on day $t - t_0 = 1$, the mass-loss rate is $\dot{M} \simeq 1.7 \times 10^{-6} [w/10 \text{ km s}^{-1}] M_\odot \text{ yr}^{-1}$. The question then arises as to the origin of this high-density stellar wind.

In a previous study of the Type Ib RSN, SN 1983N, Sramek, Panagia, & Weiler (1984) argued that the dense circumstellar cocoon was not established by the presupernova star itself, but

by a massive companion star in binary orbit with the presupernova star. Under this scenario, the progenitor stellar system involved two stars, one with zero-age main-sequence mass $M_{\text{ZAMS}} \sim 7 M_\odot$ and the other with a similar, but slightly lower mass. The more massive star in the system evolved faster to become, according to stellar evolution models (Renzini 1983), a $\sim 1.35 M_\odot$ white dwarf. At a later time, the initially less massive companion reached the RSG phase of evolution having a high mass-loss rate. It then both supplied $\sim 0.1 M_\odot$ of matter to its white dwarf companion and established a relatively high density circumstellar cocoon around the binary system. With the addition of the $\sim 0.1 M_\odot$ accreted onto the $\sim 1.35 M_\odot$ white dwarf star in the system, the white dwarf was pushed over the Chandrasekhar limit and exploded as a Type I SN. This binary system origin model for Type Ib/c explosions is then quite similar to generally accepted models for Type Ia explosions, but the modified chemical composition of the accreted surface layers of the exploding white dwarf and the interaction of its SN shock wave with the high-density circumstellar cocoon established by the RSG companion explains the observed optical and radio differences between the Type Ia and Type Ib/c SNe.

Adopting such a model for the stellar system which produced SN 1990B, we assume that the circumstellar matter was indeed due to a RSG binary companion with wind velocity $w \sim 10 \text{ km s}^{-1}$ and, therefore, that the required mass-loss rate from the companion is $\dot{M} \simeq 1.7 \times 10^{-6} M_\odot \text{ yr}^{-1}$. If this model is appropriate for Type Ic SNe in general, then the RSG wind would have to be hydrogen-poor, but not necessarily hydrogen-less in all cases, since observations suggest that some Type Ic SNe may show weak hydrogen lines in their early-time optical spectra (Filippenko 1991b).

While a binary system origin is not necessarily the only possible model for Type Ib/c SNe, the suggestion by others that Type Ib/c SNe originate from isolated massive stellar progenitors such as Wolf-Rayet stars (e.g., Fransson & Chevalier 1989; Swartz & Wheeler 1991) appears unlikely. A Wolf-Rayet star has such a fast wind that pressure from this wind would have overcome that of the RSG wind by orders of magnitude and would have swept away the high-density circumstellar material required for production of the observed radio emission. Also, the rapid development of the optical light curve for Type Ib/c SNe requires a relatively small radius ($R \ll 10^{13} \text{ cm}$) and a moderate mass ($M \lesssim 4 M_\odot$) for the SN progenitor star at the time of explosion. Such values are much smaller than the estimated properties of Wolf-Rayet stars. Such a compact SN progenitor also could not be responsible for the high-density circumstellar material implied by the observed radio emission, which requires $\dot{M}/w > [10^{-6} M_\odot \text{ yr}^{-1}/10 \text{ km s}^{-1}]$. Thus, we return to the binary system model where the dense circumstellar cocoon was established by a close RSG companion which shared a common envelope with the white dwarf progenitor to SN 1990B.

A possible binary system origin is also supported by recent theoretical models describing the optical data for Type Ib and Ic SNe (Hachisu et al. 1991). Hachisu et al. propose that both SN types result from the collapse of helium stars with mass ranges $\sim 4\text{--}6 M_\odot$ (Type Ib) and $\sim 3\text{--}4 M_\odot$ (Type Ic), having evolved from stars in binary systems with ZAMS masses of $\sim 15\text{--}20 M_\odot$ and $\sim 12\text{--}15 M_\odot$, respectively (Shigeyama et al. 1990). It should be noted, however, that such ZAMS masses are considerably higher than what the radio data appear to indicate, and that the progenitor mass range for Type Ib SNe

TABLE 8
COMPARISON OF PARAMETERS FOR RSNs 1990B, 1983N, 1984L, 1979C, AND 1986J

Parameter (1)	SN 1990B ^a (2)	SN 1983N ^b (3)	SN 1984L ^c (4)	SN 1979C ^d (5)	SN 1986J ^e (6)
SN Type	Ic	Ib	Ib	II	II
K_1	198	4400	275	1446	6.7×10^5
α	-1.12	-1.03	-1.01	-0.74	-0.67
β	-1.27	-1.59	-1.48	-0.78	-1.18
K_2	1.5×10^4	5.3×10^2	6.9×10^2	3.64×10^7	3×10^5
δ^f ($\equiv \alpha - \beta - 3$)	-2.85	-2.44	-2.53	-2.96	-2.49
Deceleration index m^f ($R \propto t^m$)	0.95	0.81	0.84	0.99	0.83
Ejecta density profile n^f ($\rho_{\text{ejecta}} \propto r^{-n}$)	~ 22	~ 7	~ 8	~ 80	~ 8
\dot{M}^g ($M_{\odot} \text{ yr}^{-1}$)	1.7×10^{-6}	9.1×10^{-7}	8.3×10^{-7}	1.2×10^{-4}	2.4×10^{-4}
Distance ^h (Mpc)	17	5	19	17	10
6 cm spectral luminosity on day 1 ⁱ ($\text{ergs s}^{-1} \text{ Hz}^{-1}$)	7×10^{28}	1×10^{29}	1×10^{29}	5×10^{29}	8×10^{31}

^a Parameters are from Table 7 of this paper.

^b Parameters are from Weiler et al. 1986 for a four-parameter fit.

^c Parameters are from Panagia et al. 1986, adopting the Chevalier model ($\delta = \alpha - \beta - 3$; Chevalier 1984b) and fitting K_1 , α , β , and K_2 as free parameters.

^d Parameters are from Weiler et al. 1991.

^e Parameters are from Weiler et al. 1990.

^f Parameters δ , m , and n are related by $\delta = -3m = -3(n-3)/(n-2)$ for a circumstellar wind gas density distribution $\rho_{\text{wind}} \propto r^{-2}$, a shock front radius R increasing with time as $R \propto t^m$, and an optical depth $\tau \propto R^{-3}$.

^g The mass-loss rate \dot{M} was calculated using eq. (16) of Weiler et al. (1986) assuming an RSG wind velocity $w = 10 \text{ km s}^{-1}$, ejecta expansion velocity $v_i = 10^4 \text{ km s}^{-1}$ on day $t_i = 45$ days, and a RSG wind temperature $T = 10^4 \text{ K}$. The parameter m is defined above, and the optical depth at 5 GHz, $\tau_{5 \text{ GHz}}$, is taken to be K_2 on $t - t_0 = 1$ day.

^h Distances d to the RSN parent galaxies NGC 4568 (1990B), NGC 5236 (1983N), NGC 991 (1984L), NGC 4321 (SN 1979C), and NGC 891 (SN 1986J) are from Tully (1988) with $H_0 = 75 \text{ km s}^{-1} \text{ Mpc}^{-1}$.

ⁱ The radio spectral luminosities at 6 cm are defined as $4\pi d^2 K_1$. Note that these are *not* observed values but are formal model values for the luminosity at 5 GHz 1 day after explosion.

compared to the range for Type Ic SNs inferred by Hachisu et al. (1991) and Shigeyama et al. (1990) is the reverse of what is implied by the radio data (i.e., we argue in § 6.3 that the progenitor binary systems for Type Ic SNs should be more massive than the progenitor binary systems for Type Ib SNs).

6.2. Comparison of Type Ib/c and Type II RSNs

A companion is given in Table 8 of the model parameters and calculated physical properties for SN 1990B with those estimated for the Type Ic RSNs, SN 1983N (Sramek et al. 1984; Weiler et al. 1986) and SN 1984L (Panagia et al. 1986). Examination of Table 8 shows that the spectral indices α are the same to within the errors for all three objects and the decline rates β are similar, but are slightly steeper for SN 1983N and SN 1984L than for SN 1990B. Also given in Table 8 are estimated distances (Tully 1988; with $H_0 = 75 \text{ km s}^{-1} \text{ Mpc}^{-1}$) to each of the RSNs and absolute radio spectral luminosities based on the values for the formal, model 6 cm radio spectral luminosities 1 day after explosion ($4\pi d^2 K_1$, where d is the parent galaxy distance). The 6 cm initial spectral luminosities are very similar, with SN 1990B perhaps being slightly fainter. Note, however, that the initial 6 cm optical depths (K_2) are much lower for the two Type Ib SNs, SN 1983N and SN 1984L, than for this Type Ic SN.

Comparison of these values with those for the Type II RSNs SN 1979C (Weiler et al. 1986, 1991; Van Dyk et al. 1993) and SN 1986J (Weiler et al. 1990; Van Dyk et al. 1993), also given in Table 8, shows that Type Ib/c RSNs form a distinct class of objects from the Type II RSNs, which have generally flatter spectral indices α , slower rates of decline after maximum radio brightness β , and much higher initial optical depths K_2 . These differences imply that Type Ib/c RSNs have very different circumstellar environments from the Type II RSNs and therefore

very different progenitor systems from the exploding isolated RSG origin expected for Type II RSNs.

6.3. Comparison of Type Ib and Type Ic RSNs

By definition Type Ic SNs are helium-poor in their optical lines in comparison with Type Ib SNs. Also, even though the Type Ib and Type Ic RSNs are quite similar in their radio properties and are clearly distinguishable in their radio emission from Type II RSNs, closer examination of Table 8 shows significant differences between the Type Ic RSN, SN 1990B, and the two Type Ib RSNs, SN 1983N and SN 1984L.

Keeping in mind the dangers of small-number statistics, with only 1 Type Ic RSN and 2 Type Ib RSNs available for comparison, it appears that the Type Ic RSN, SN 1990B, may have turned on more slowly at 6 cm ($\sim 38 \pm 14$ days from explosion to 6 cm maximum) than did the Type Ib RSN, SN 1983N ($\sim 16 \pm 1$ days from explosion to 6 cm maximum). This turn-on time is directly related to the model value for the initial 6 cm optical depth, K_2 , which is significantly higher for SN 1990B than for SN 1983N or SN 1984L. Correspondingly, the mass-loss rate (\dot{M}) from the presupernova system is higher for SN 1990B, possibly implying, under the binary origin model, a more massive RSG companion to the presupernova star.

In addition, the ejecta from SN 1990B appears to be less decelerated (the shock front radius increases with time according to $R \propto t^m$ [Chevalier 1982a, b], and for free-free absorption $\tau \propto R^{-3}$, the deceleration index $m = -\delta/3 \sim 0.95$ for SN 1990B, while $m \sim 0.8$ for SN 1983N and SN 1984L) with a steeper density profile (the SN ejecta density profile $\rho_{\text{ejecta}} \propto r^{-n}$, so $\delta = -3(n-3)/(n-2)$ [Chevalier 1982a, b], and thus $n \sim 22$ for SN 1990B, while $n \sim 7-8$ for SN 1983N and SN 1984L) than is true for the two Type Ib RSNs. This suggests that, while the Type Ib/c SNs have many similarities and are

significantly different as a group from Type II SNe in terms of their radio properties, there may also be distinguishable differences, and therefore progenitor system variations, between the Type Ib and Type Ic RSN subclasses. More observations are obviously needed to confirm these subclass differences.

Finally, it is interesting to note that the absolute 6 cm radio spectral luminosities based on the values for K_1 are identical for SN 1983N and SN 1984L and very similar to the value for SN 1990B. This consistency in the radio spectral luminosity implies that the circumstellar environments and the interaction of the SN shocks with these environments are quite similar for all three RSNs. Such a similarity suggests that Type Ib, and possibly Type Ib/c SNe, may be useful as radio "standard candles" and may provide a class of known luminosity radio emitters.

7. CONCLUSIONS

Analysis of the radio emission from the Type Ic radio supernova SN 1990B at 20, 6, and 3.6 cm leads to the following conclusions:

1. The behavior of the radio emission from SN 1990B is regular in nature.
2. The light curves are consistent with the model for non-thermal emission with external, thermal absorption which was applied earlier to the Type Ib SNe 1983N and 1984L and to such Type II SNe as SN 1979C.

3. The radio properties of SN 1990B are quite similar to those of the Type Ib SNe 1983N and 1984L, and quite different from the Type II RSNs such as SN 1979C and SN 1986J. This strongly suggests that Type Ib/c RSNs constitute a related group.

4. Our preferred model for the Type Ib/c progenitor systems is an interacting binary with stellar components in the ZAMS mass range $\sim 6\text{--}8 M_{\odot}$. The suggestion by other authors of a Wolf-Rayet star origin for Type Ib/c SNe appears untenable (cf. § 6.1).

5. In spite of their basic similarities, Type Ib and Type Ic SNe may be distinguishable in their radio emission and physical properties, with the Type Ic RSNs originating in an environment with a higher mass-loss rate from the RSG companion, less deceleration of the ejecta, and a steeper ejecta density profile than is found for the Type Ib RSNs (cf. § 6.3).

6. Although limited by our sample of only three objects, it appears that Type Ib RSNs, and possibly both Type Ib and Type Ic RSNs, may be "standard candles" in their 6 cm radio emission and, if confirmed, constitute the first and only such targets available for purely radio distance determinators.

We would like to thank A. Miocluszewski for early work on the radio observations of this SN.

REFERENCES

- Abramowitz, M., & Stegun, I. A. 1965, *Handbook of Mathematical Functions* (NY: Dover), 980
- Benetti, S., Capellaro, E., & Turatto, M. 1990, *IAU Circ.*, No. 4967
- Chevalier, R. A. 1981a, *ApJ*, 246, 267
- . 1981b, *ApJ*, 251, 259
- . 1982a, *ApJ*, 259, 302
- . 1982b, *ApJ*, 259, L85
- . 1984a, in *11th Texas Symposium on Relativistic Astrophysics*, ed. D. S. Evans (*Ann. NY Acad. Sci.* No. 422, 215)
- . 1984b, *ApJ*, 285, L63
- Dopita, M. A., & Ryder, S. D. 1990, *IAU Circ.*, No. 4953
- Filippenko, A. V. 1990, *IAU Circ.*, No. 4953
- . 1991a, in *SN 1987A and Other Supernovae*, ed. I. J. Danziger & K. Kjar (*Garching bei Munchen: ESO*), 343
- . 1991b, *IAU Circ.*, No. 5169
- Fransson, C., & Chevalier, R. A. 1989, *ApJ*, 343, 323
- Hachisu, I., Matsuda, T., Nomoto, K., & Shigeyama, T. 1991, *ApJ*, 368, L27
- Hjellming, R. M., & Bignell, R. C. 1982, *Science*, 216, 1279
- Jeffery, D. J., Branch, D., Filippenko, A. V., & Nomoto, K. 1991, *ApJ*, 377, L89
- Kirshner, R. P. 1990, in *Supernovae*, ed. A. G. Petschek (New York: Springer), 59
- Kirshner, R., & Leibundgut, B. 1990, *IAU Circ.*, No. 4953
- Napier, P. J., Thompson, A. R., & Ekers, R. D. 1983, *Proc. IEEE*, 71, 1295
- Panagia, N., Sramek, R. A., & Weiler, K. W. 1986, *ApJ*, 300, L55
- Panagia, N., Cassatella, A., Gonzalez-Riestra, R., Talavera, A., & Wamsteker, W. 1990, *IAU Circ.*, No. 4959
- Perlmutter, S., & Pennypacker, C. 1990, *IAU Circ.*, No. 4949
- Phillips, M. M., & Ruiz, M.-T. 1990, *IAU Circ.*, No. 4959
- Renzini, A. 1983, in *IAU Symp. 103, Planetary Nebulae*, ed. D. R. Flower (Dordrecht: Reidel), 267
- Shigeyama, T., Nomoto, K., Tsujimoto, T., & Hashimoto, M. 1990, *ApJ*, 361, L23
- Sramek, R. A., Panagia, N., & Weiler, K. W. 1984, *ApJ*, 285, L59
- Sramek, R. A., Weiler, K. W., & Panagia, N. 1990, *IAU Circ.*, No. 4979
- Suntzeff, N. 1990, *IAU Circ.*, No. 4959
- Suntzeff, N., & Phillips, M. 1990, *IAU Circ.*, No. 4961
- Swartz, D. A., & Wheeler, J. C. 1991, *ApJ*, 379, L13
- Thompson, A. R., Clark, B. G., Wade, C. M., & Napier, P. J. 1980, *ApJS*, 44, 151
- Tully, R. B. 1988, *Nearby Galaxies Catalog* (Cambridge: Cambridge Univ. Press)
- Van Dyk, S. D., Weiler, K. W., Panagia, N., & Sramek, R. A. 1993, in preparation
- Weiler, K. W., Panagia, N., & Sramek, R. A. 1990, *ApJ*, 364, 611
- Weiler, K. W., & Sramek, R. A. 1988, *ARA&A*, 26, 295
- Weiler, K. W., Sramek, R. A., Panagia, N., van der Hulst, J. M., & Salvati, M. 1986, *ApJ*, 301, 790
- Weiler, K. W., Van Dyk, S. D., Panagia, N., Sramek, R. A., & Discenna, J. L. 1991, *ApJ*, 380, 161
- Wheeler, J. C., & Harkness, R. 1990, *Rept. Progr. Phys.*, 53, 1467